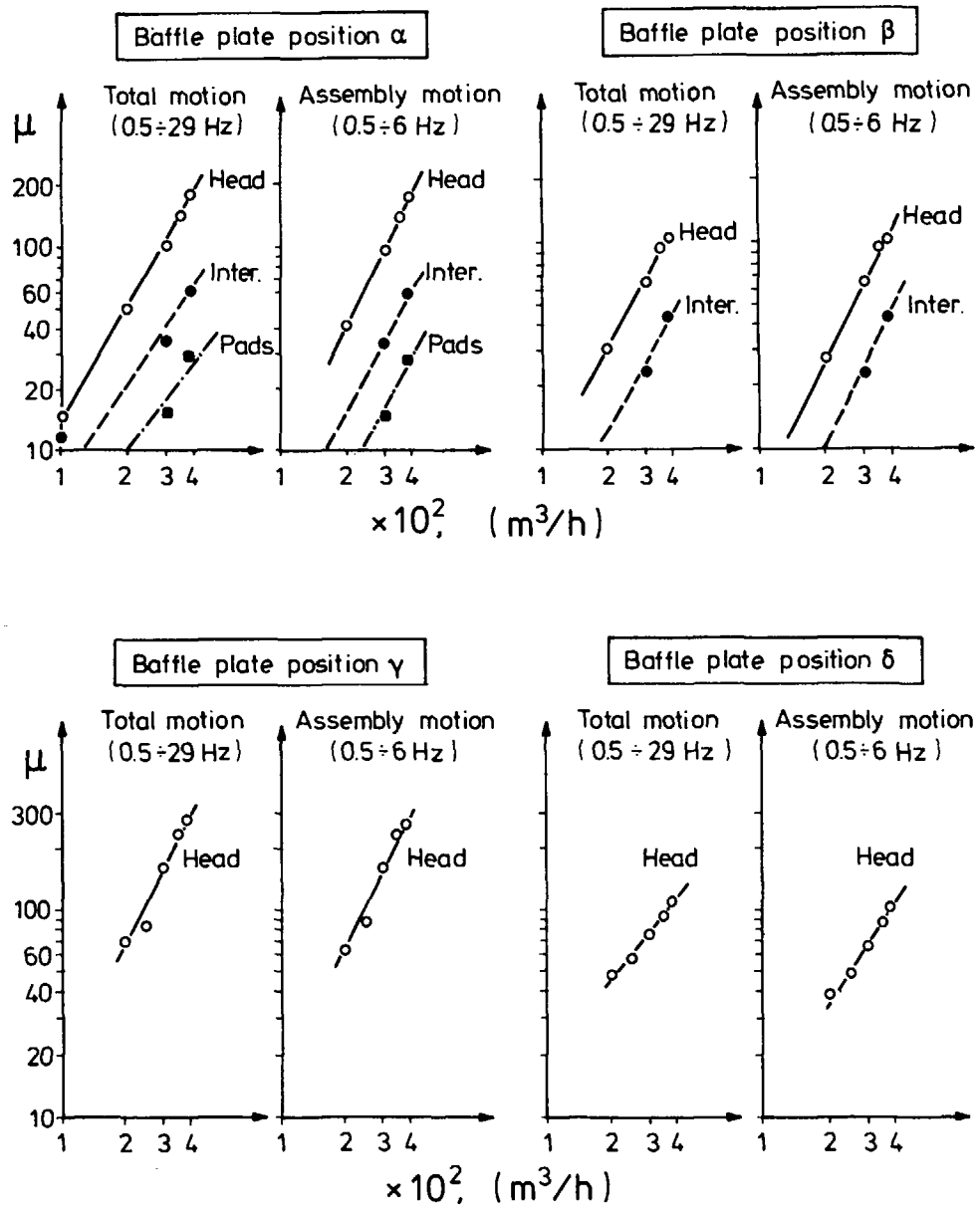

Fig. 34 – R.M.S. (in μ) of vibration at some levels of "E„ fuel bundle versus flow rate.

Analysis of Flow Induced Vibration in Heat Exchangers by A. W. van Beek, Netherlands.

ABSTRACT

A description will be given of three different types of heatexchangers developed by the Dutch Nuclear Industry Group "Neratoom" in cooperation with TNO for the sodium-cooled fast breeder reactor SNR-300 at Kalkar. Moreover, the research related with flow induced vibrations carried out by TNO (Organization for Applied Scientific Research) will be presented.

The flow induced forces on the tubes of the straight-tube steamgenerators were measured at the inlet and outlet section where partial cross-flow occurs. With the measured flow induced forces the response of a tube was calculated as a function of the tube-to-supportbush clearances taking into account the non-linear damping effects from the sodium.

The theoretical results showed that for this particular design no tube impact damage is to be expected which was confirmed later by a full scale experiment.

Special attention will be devoted to the steamgenerator with helical-coil tube-bundles, where the sodium flows in a counter cross-flow over the tube-bundle. Extensive measurements of the power spectra of the flow induced forces were carried out since no information could be found in the literature. The vibration analysis will be presented and vibration modes of the entire bundle will be compared with experimentally obtained results.

Finally a description of the vibration tests to be carried out on the intermediate heatexchanger (IHX) will be presented.

1. INTRODUCTION

The Dutch Nuclear Industry Group B.V. Neratoom participate in the De-BeNeLux Consortium "Internationale Natrium-Brut-Reaktor-Bau Gesellschaft m.b.H. (INB), founded in 1972 by the German, Belgian and Dutch Industries.

This Consortium received the order to design and build the prototype sodium-cooled fast breeder reactor SNR-300, at Kalkar.

The SNR-300 is a loop-type reactor, with three primary and three secondary loops. The heat, which is generated in the reactor, is transferred by 9 intermediate heatexchangers (3 in each loop) to the secondary circuits. Two of the secondary circuits are equipped with 3 straight-tube steamgenerators.

In the DeBeNeLux SNR-300 project Neratoom is responsible for the development and delivery of steamgenerators, intermediate heatexchangers (IHX) and sodium pumps, which are built in the fabrication facilities of "Stork" and "De Schelde" in the Netherlands.

Experiments to determine the flow induced fluctuating forces on the steamgenerator tubes were carried out by TNO with large models in a water test circuit and extensive response analyses were carried out to ensure that no excessive vibrations will occur under operating conditions.

From the end of 1971 until June 1974 a 50 MW prototype straight tube steamgenerator was tested during over 3000 hours in the Dutch 50 MW sodium component test facility. After the end of the tests the evaporator was dismantled for detail inspection, while the superheater is still in operation for further testing. From January 1974 till January 1975 a helical-coil evaporator was tested for 3000 hours. This evaporater was dismantled, inspected and reassembled and has been taken into operation again for further tests. During the inspections no major problems were detected.

2. STRAIGHT-TUBE STEAMGENERATORS

In the straight tube-steamgenerator, shown in Fig. 1, the sodium flows from the upper inlet-nozzle through a perforated plate for the proper distribution of flow in the upper part of the flow-shroud, downwards on the outside of the tubes, thus transferring its heat to the water/steam, which flows in a counter flow direction on the inside of the tubes.

The tube sheets are connected by single-length straight tubes, which are internal-bore welded to the tube sheets. A carefully designed tube support structure has been applied which allows the sodium to flow parallel through the tube-bundle, thereby minimising the effects of flow induced vibrations.

A hexagonal flow shroud around the tube-bundle is used to restrict the sodium flow. The difference in the thermal expansion between shell and tube-bundle is compensated for by bellows in the shell.

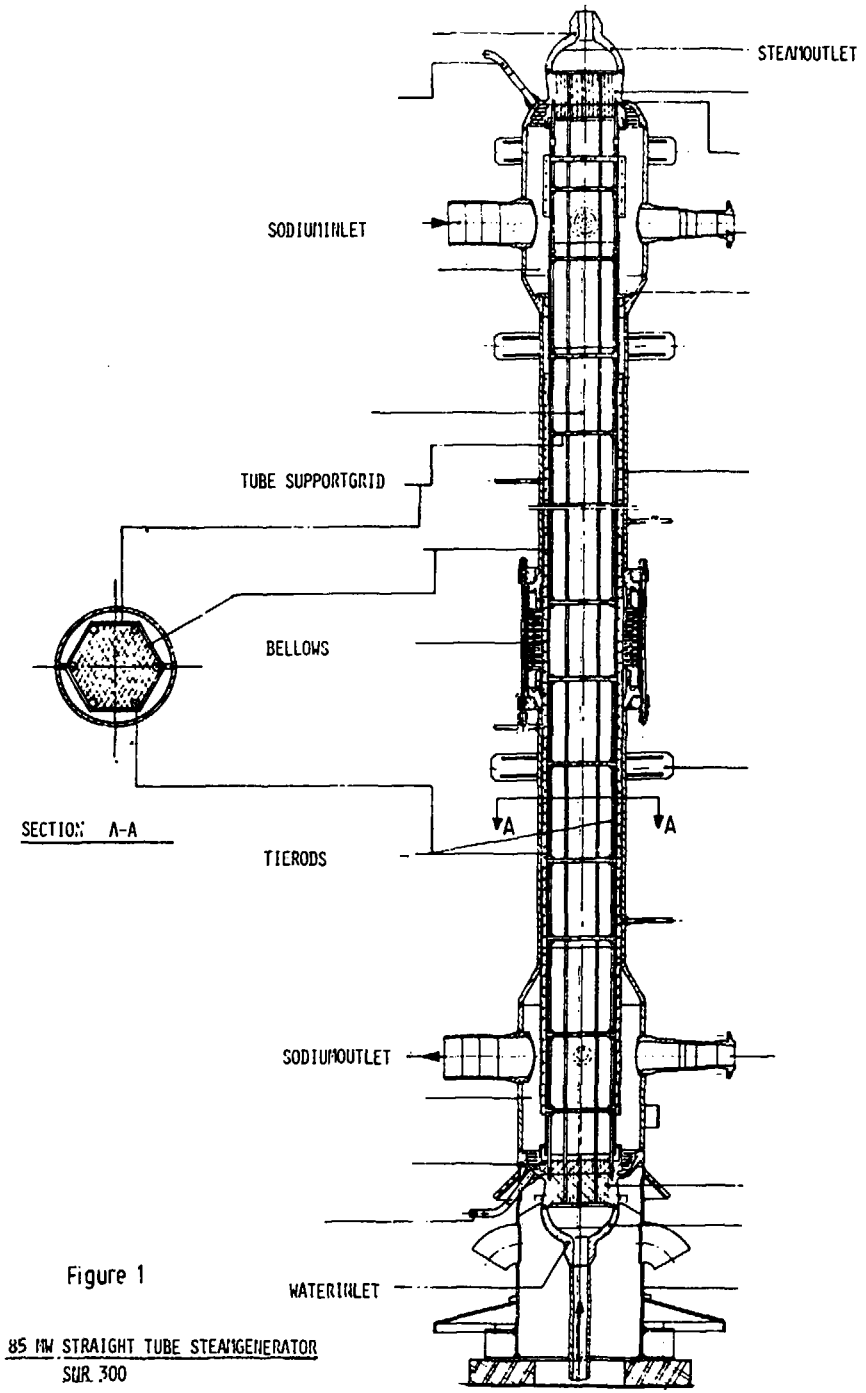

Figure 1

85 MW STRAIGHT TUBE STEAMGENERATOR
SUR 300

The main dimensions of the evaporator and superheater are given in Table 1.

TABLE 1
STEAMGENERATOR DIMENSIONS

	Evaporator		Superheater	
	Prototype	SNR 300	Prototype	SNR 300
Tube diameter x wallthickness [mm]	17.2x2.3	17.2x2	17.2x2.9	17.2x2.9
Pitch [mm]	27.5	30	27.5	30
Number of tubes	139	211	139	211
Tube length between tube plates [m]	19.34	20	14.58	15.3

2.1. Measurement of flow induced forces.

For the straight tube steamgenerator excitation of the tubes is caused at the inlet and outlet section of the sodium where partial cross flow occurs. With a model of these sections trials were done to assess the excitational forces induced by the liquid. Results of these trials were used to determine the vibrational behaviour of the steamgenerator under operational conditions.

2.1.1. Description of the experimental hydraulic model.

The experiments were carried out in a closed loop flow circuit, a diagram of which is shown in Fig. 2. The figure also shows the spot where the model of the sections to be used is placed.

For both the inlet and the outlet sections the same model was used, of course reversely installed.

Fig. 3 shows a diagram of this model which is in fact only a 60^{o} sector of a section.

The locations of the measuring tubes are also shown in Fig. 3. During the experiments the influence of perforated plates on the excitational forces was investigated.

For the experiments water was used at a Reynolds number equalling the Re in the steamgenerator proper at operating conditions (2x $10.^{5}$). At this Re number the geometry of the model was chosen in such a way that the frequency of the vortices leaving the tubes was half the value of the natural frequency of the measuring tube in order that no excessive deflections were created. This resulted in an enlarged model (scale 2 : 1).

Three measuring tubes were used installed in the 1st, 2nd and 3rd row (see Fig. 3). These tubes were stiffly attached to the tube sheet at one end and could move freely at the other. Near the attachment to the tube sheet the measuring tubes were provided with strain gauges with which the bending moment on the tube in flow direction and perpendicular to it could be measured. By calculation these moments were converted to forces per unit length of the tube.

During the experiments the water flow rate, pressure drop and water temperature were also measured.

The influence of three types of perforated plates on the vibrational behaviour of the tubes was investigated during the experiments.

2.1.2. Average forces on the tubes.

From the measured data the average bending moments in flow direction and perpendicular to it and from these the average forces on the measuring tubes were calculated.

The presence of perforated plates greatly reduced the forces excited on the tubes. No significant difference in performance of the different plates could be found.

2.1.3. Power spectral density.

Also the power spectral density of the fluctuating forces as a function of the Strouhal number ($S = \frac{fd}{v}$ in which d = tube outer diameter, v = flow velocity and f = frequency) were measured.

In both direction: x-direction (flow direction) and y-direction (perpendicular to flow direction) the spectra leveled off at 40-45 Hz to zero. Again the shape of the spectra was hardly influenced by the type of plate. It turned out that as outlet section much less vibrational force was induced then in case the model was used as inlet section. Fluctuating forces in x-direction can be neglected as compared to those in y-direction.

A typical example of a power spectral density plot is given in Fig. 4.

The symbols used are:

f = frequency $[s^{-1}]$

$K_y(f)$ = power spectral density of fluctuating force in y-direction per unit length $[N^2s/m^2]$

$\bar{K}_x$ = average force per unit length in x-direction $[N/m]$.

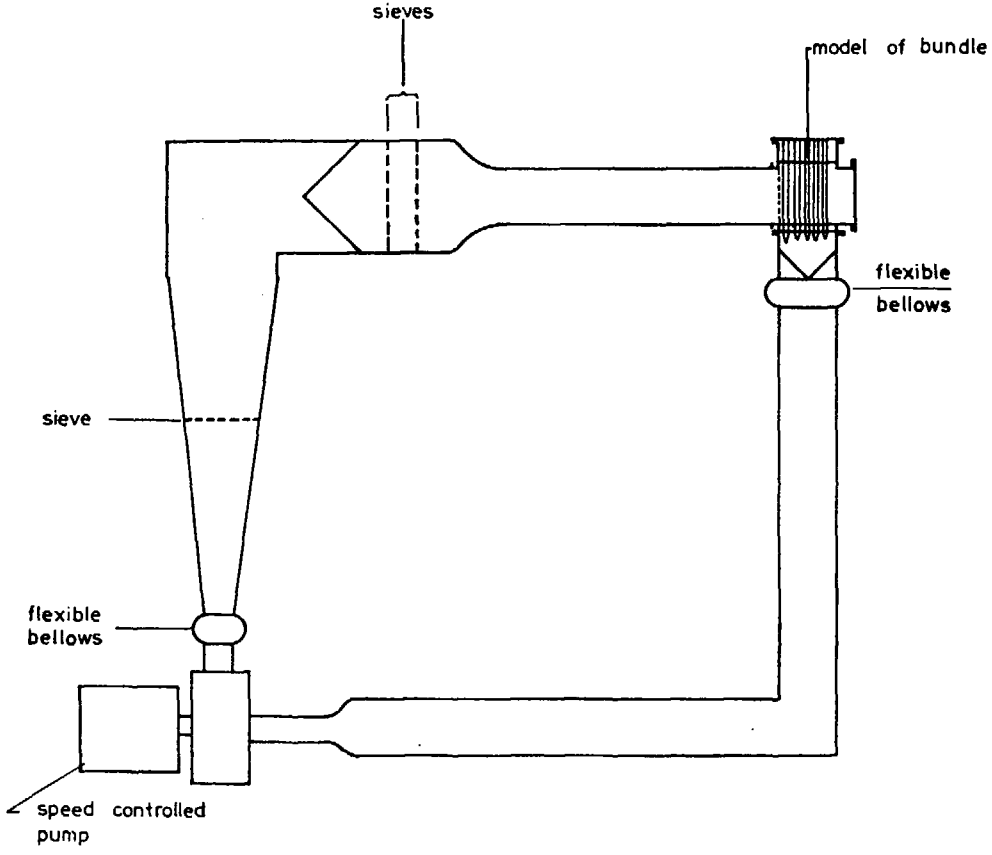

Figure 2 Water test circuit

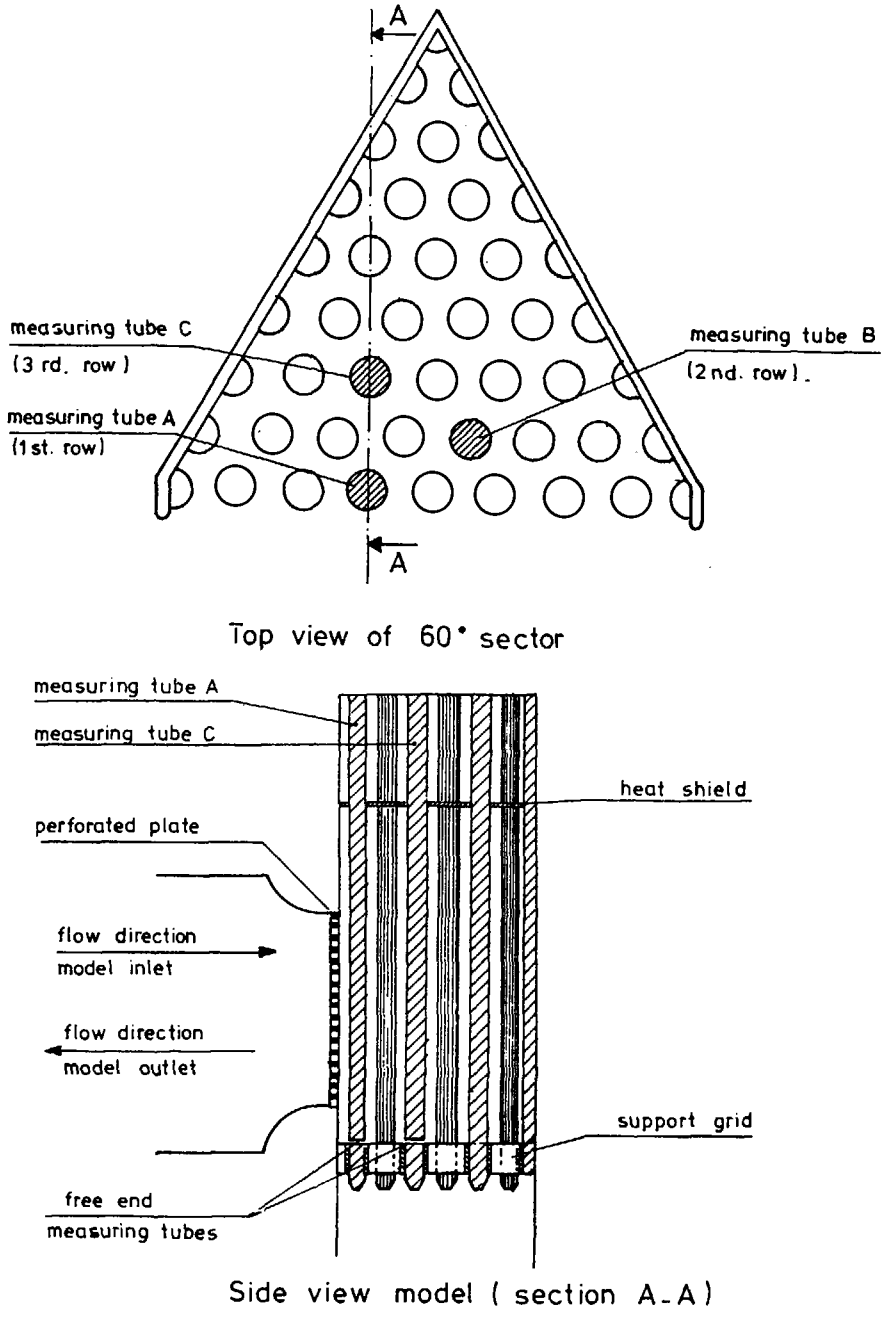

Figure 3 Model of inlet and outlet section of tube bundle.

2.1.4. Effective lift coefficients.

For the vibration analysis the narrow-band random excitation forces were simulated by sinusoidal excitation.

The rms response of a structure to a narrow-band random excitation of given rms value is the same as for a sinusoidal of the same rms value. When a band is "narrow" is determined by the damping of the responding structure. It should certainly be less than the width of a resonance amplification curve of the structure at half-maximum value.

However, the procedure will be conservative if the band is not narrow.

The fluctuating forces per unit length of the tube were defined by:

$$q_y = C_\ell \cdot \tfrac{1}{2}\rho\, v^2 d \cos\omega t \quad , \qquad (1)$$

where

ρ = density of the sodium

C_ℓ = effective lift coefficient

ω = circular frequency

t = time.

2.2. Response analysis of the straight steamgenerator tubes.

The steamgenerators under consideration are provided with very long straight tubes and a large number of tube-support-grids. The distance between the support-grids is chosen so that the lowest natural frequency of a tube, that is simply supported at its support-grids, is well above the excitation frequency associated with the highest sodium flow.

Consequently the vibrations will be very small provided that the support conditions are available. Since the tubes have clearances within the support-grid holes because of manufacturing requirements, the tubes may be completely free from the support-grids and have natural frequencies within the excitation frequency spectrum. Therefore, it will be necessary to calculate the vibrational behaviour of the tubes under various resonant conditions. The main parameters governing the maximum amplitude of vibration are the magnitude of the excitation forces and the damping of the system, which is significantly influenced by the clearance of the tube in the support-grid holes. The purpose of this analysis was to investigate the influence of the tube support clearance on the vibrational behaviour.

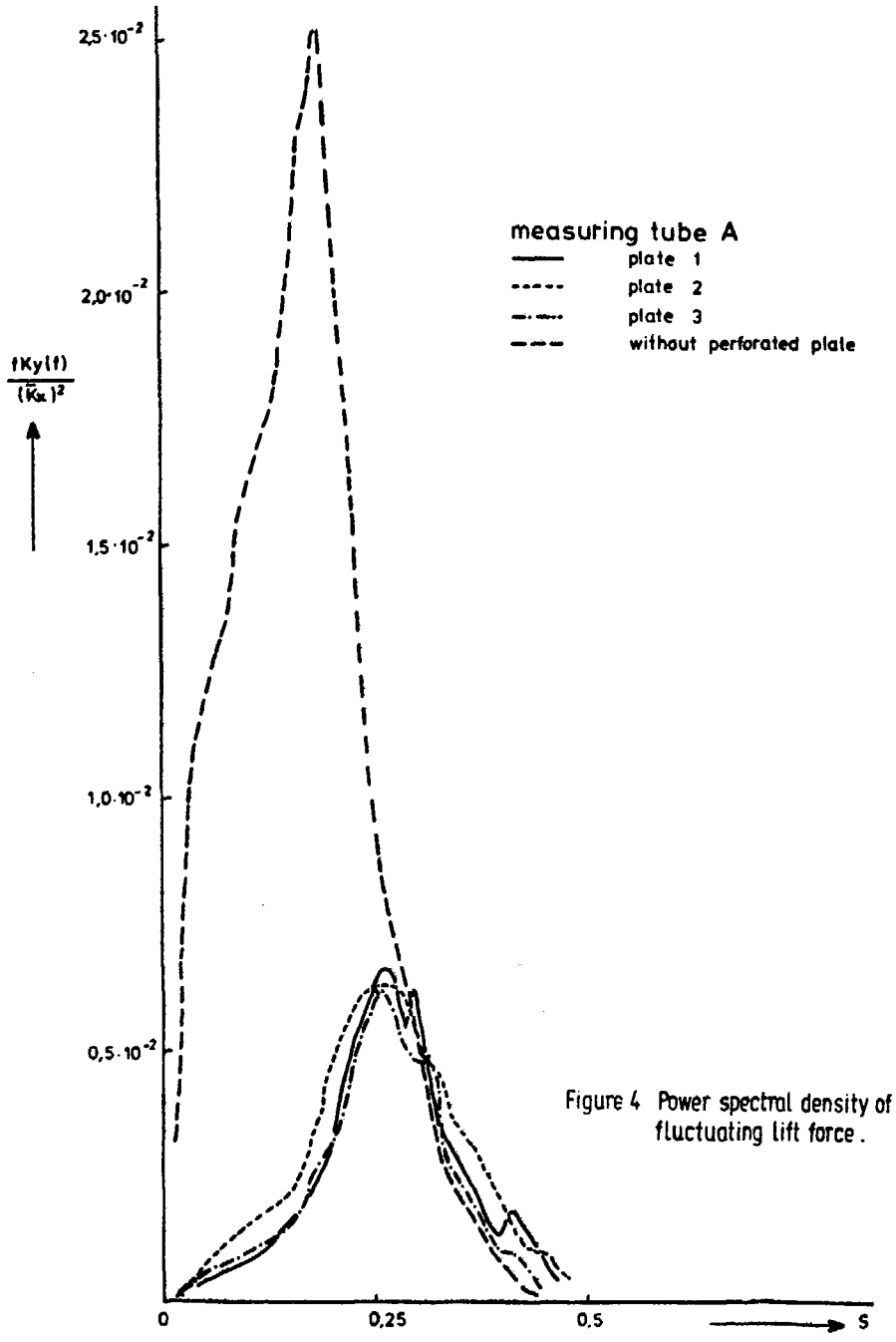

Figure 4 Power spectral density of fluctuating lift force.

2.2.1. Natural frequencies and vibration modes.

The natural frequencies and vibration modes can readily be calculated taking into account the added mass of the liquid and the tension load on the tube. The calculations were based on the assumption that the tube is free from the support-grids. The support-grids behave than as dash-pot elements.

A large number of natural frequencies of the tubes were found within the possible excitation frequency range.

2.2.2. Damping.

The response of the tube, excited by fluctuating forces with frequencies that can coincide with a natural frequency can only be calculated if the damping is known with sufficient accuracy.

The basic forms of damping for the tube are:

- structural damping
- viscous damping in the support-grid holes
- hydrodynamic damping due to drag forces.

The effect of the structural damping in the straight tubes appeared to be negligible in comparison with the other forms of damping. The damping in the support-grids can be accounted for with dash-pot elements as shown in Fig. 5. The damping coefficients depend on diameter, length and clearance of the support, the viscosity of the sodium, and the relative eccentricity of the tube. The smallest value for the damping coefficient will be obtained for zero eccentricity and therefore, the analysis was carried out with this assumption.

If the tube vibrates in molten sodium then the sodium will exert drag forces on the tube. This form of damping will become important if large clearances between tube and support-grids have to be applied. If $\dot{u}_y(\frac{z}{\ell})$ denotes the lateral velocity of the tube at the relative position z/ℓ as a consequence of the vibration then the damping force per unit length of the tube, q, was approximated by:

$$q_y(\tfrac{z}{\ell}) = -c_D \cdot \tfrac{1}{2} \rho \dot{u}_y(\tfrac{z}{\ell}) \cdot |\dot{u}_y(\tfrac{z}{\ell})| \cdot d \quad , \qquad (2)$$

where c_D is the drag coefficient
ρ is the density of the sodium
d is the tube diameter.

This form of non-linear damping has been taken into account by calculating the work dissipated per cycle, assuming sinusoidal motion.

2.2.3. Response at resonance frequency.

From the measurement of the excitation forces followed that the fluctuating forces at the outlet section can be neglected in comparison with those forces at the inlet section.

The maximum amplitude of the tube has been calculated for a number of resonance frequencies by calculation of the work done per vibration period by the excitation forces and the work dissipated per period by the damping forces.

With this method non-linear damping can easily be taken into account.

Figure 6 shows for the highest sodium flow the calculated maximum relative displacement of the evaporator tube in a support bush as a function of the relative clearance. It is clearly shown that for this particular design no tube impact damage is to be expected.

2.3. Measurements on tubes of prototype steamgenerator (50 MW).

In this component measurements were carried out with a pick-up, which was placed in the innerside of the tube. This pick-up could be moved in the tube and fixed on a desired place by means of air-pressure.

The pick-up was equipped with 2 acceleration units, with their axes perpendicular to each other.

The measurements were carried out at full sodium flow in 4 tubes at different levels.

Maximum amplitudes were measured at frequencies of 50, 75, 135 and 365 Hz. The amplitudes were very small (2×10^{-9} m).

It appears that the amplitudes over the tube length were of the same magnitude as in the inlet region.

3. THE 50 MW HELICAL-COIL STEAMGENERATOR

In addition to straight tube steamgenerators Neratoom and partners decided in 1970 to develop a second type of steamgenerator: the helical tube type. It was intended to be used in the SNR-300 together with the straight type to investigate which type has the greatest potentials.

In the steamgenerator with helical-coil tube bundle, water/steam flows from the inlet header on the lower part of the unit through helical-coiled tubes within the shell in an upward direction and leaves the

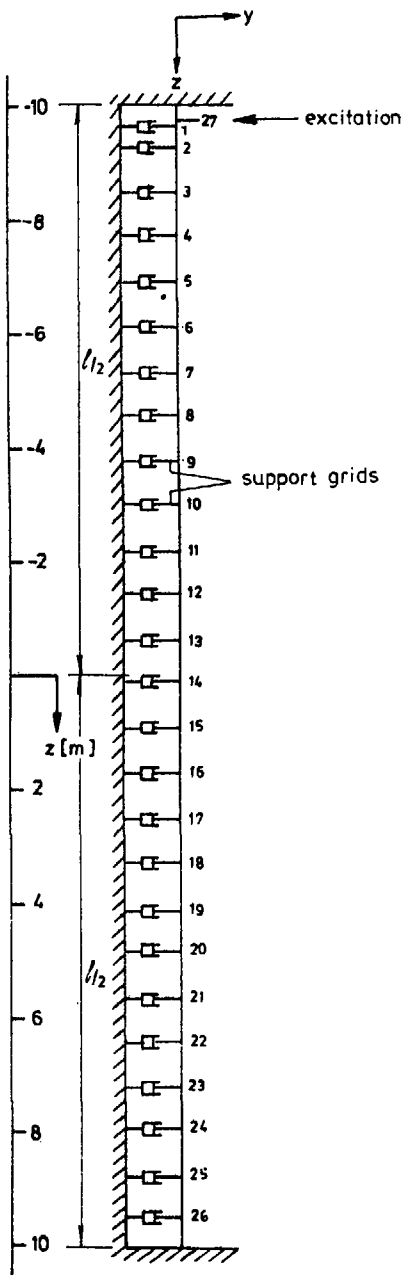

Figure 5

Model of evaporator tube for response analysis.

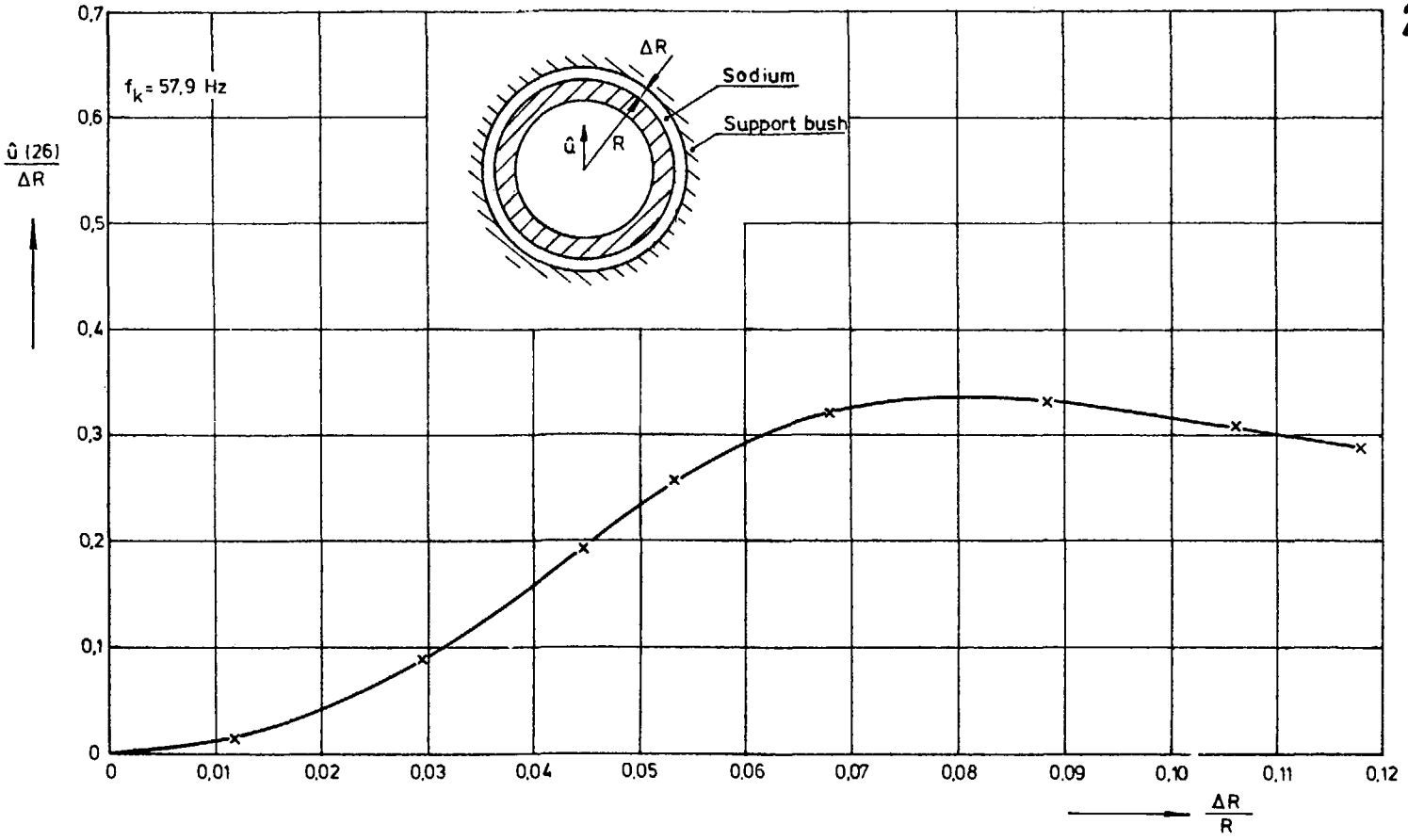

Figure 6 The calculated maximum relative displacement of the evaporator tube in the support bush as a function of the relative clearance.

unit through the upper-outlet header as shown in figure 7. Sodium flows in a counter cross-flow over the tube bundle in a downward direction.

The bundle consists of various layers of helical tubes, supported by vertical tie-bars. Each layer can expand freely in a vertical direction. Both ends of each helical tube passes through the upper- and lower-half globes of the shell by the application of thermal sleeves.

The individual tubes are then connected externally with water/steam headers.

The main dimensions of the evaporator and superheater are given in Table 2.

3.1. Measurement of excitational forces.

In the helical coiled steamgenerator the sodium flows in cross flow through the bundle, the latter being composed of rings of helices which are alternately wound in clockwise and counterclockwise direction. For this configuration the frequency and the magnitude of the fluctuating forces which are exerted on the tubes by the sodium flow can neither be determined with sufficient accuracy from literature nor from calculations.

The aim of the investigations was: provision of experimental data for the determination of the vibrational behaviour of the tubes of the helically coiled steamgenerator.

TABLE 2
DIMENSIONS OF HELICAL-COIL STEAMGENERATORS

		Evaporator		Superheater
		Prototype	SNR 300	SNR 300
Tube diameter x wallthickness	[mm]	25.0x2.6	26.9x2.9	26.9x4.5
Tube length in the bundle	[m]	42	40.56	30.74
Number of tubes		100	77	77
Number of concentric bundles		8	7	7
Shell diameter	[mm]	1370	1400	1400
Overall height	[m]	9.8	12	10.5

3.1.1. Description of the experimental hydraulic model.

The experiments for the determination of the fluctuating forces on the tubes were carried out in the water test circuit shown in Fig. 2.

The hydraulic model for the simulation of a bundle section is shown in Fig. 8. It consists of a horizontal flow channel with a rectangular cross section in which rows of straight tubes are arranged at an inclination angle of 9° with respect to the vertical. The length/dia ratio of the tube is 12.

In agreement with the alternately clockwise and counterclockwise winding direction of the helices in the steamgenerator the inclination angle of neighbouring rows of tubes in the flow model is alternately $+9^{\circ}$ and -9°.

The pitch/diameter ratios of the tubes are in longitudinal direction 1,4 and in transverse direction 1,56.

This arrangement of tube data was chosen as being sufficiently representative for the SNR-300 steamgenerator out of a set of available tube arrangements, being intended for the investigation of the fluctuating forces over a larger range of tube inclination angles and pitch/diameter ratios.

For comparison the exact data for the SNR-300 steamgenerator are:

Tube inclination angle	$8{,}6^{\circ}$
Longitudinal pitch/dia ratio	1,41
Transversal pitch/dia ratio	1,48.

In Fig. 8 the crossing points of neighbouring tubes lie in the horizontal mid-plane of the flow channel. Neighbouring tube rows can be shifted relative to each other however, so that the position of the crossing points of adjacent tubes can be varied.

For the determination of the influence of the turbulence intensity of the flow entering the bundle, perforated plates can be arranged about 10 tube diameters upstream of the bundle. The perforated plates used in the experiments are a scaled-up steamgenerator plate and a plate with coarser perforations producing a larger ratio of turbulence scale with respect to tube diameter. Also measurements were carried out without a perforated plate.

The fluctuating forces are determined by measuring the bending moment exerted by the fluctuating forces on a measuring tube. The measuring tube is a tube which is clamped at one end and free at the other end. It is provided with strain gauges. The bending moment is measured in the direction and perpendicular to the direction of the flow.

Assuming the fluctuating forces to be evenly distributed along the length of the tube and taking into account the transfer characteristics of the measuring tube the statistical characteristics of the fluctuating forces such as coherence functions and power spectral density are determined.

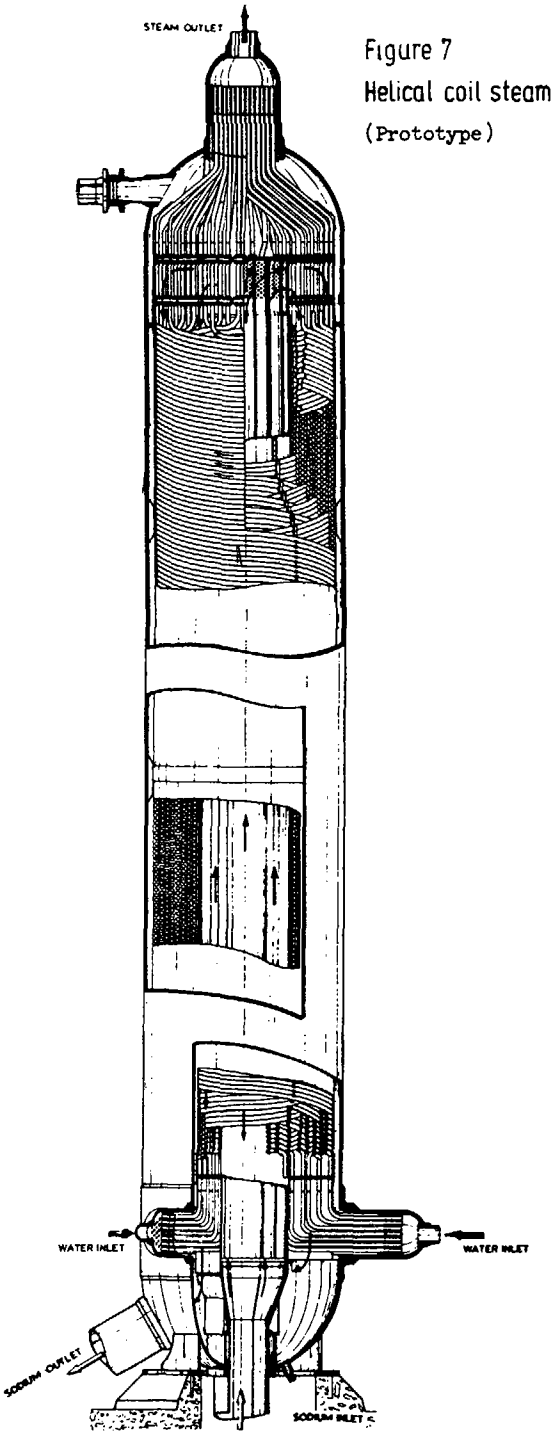

Figure 7
Helical coil steam generator
(Prototype)

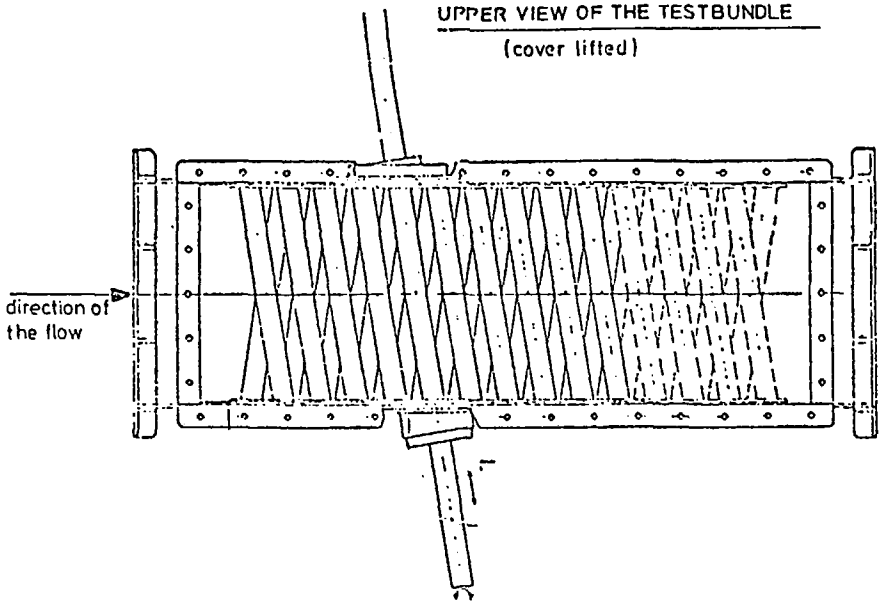

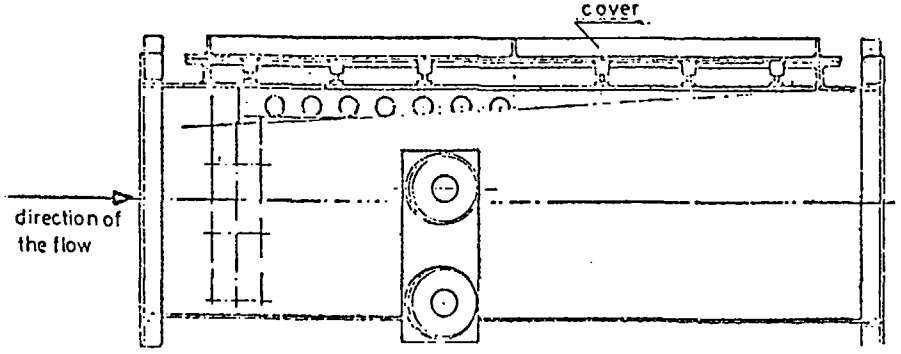

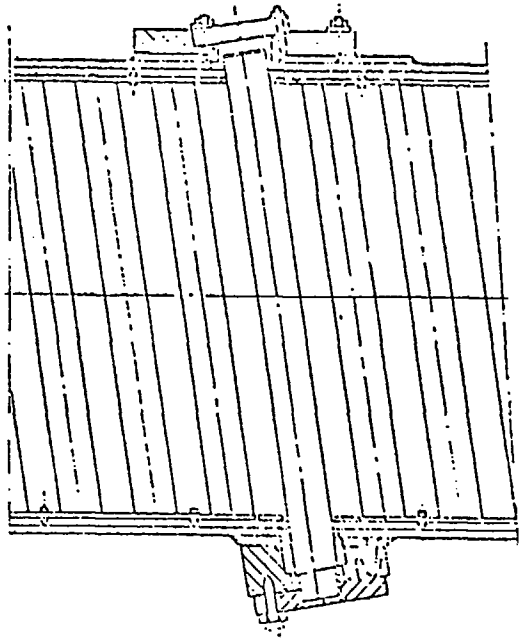

moment measuring tube mounted in
the testbundle

Figure 8
Model of section of helical coiled
tube bundles.

The number of parallel rows is 8. The number of tubes in each parallel row was 10 for the first experiments and was extended to 15 later. The measuring tube can be positioned at the following locations[+]:

- 1st bank at the position of a tube at the wall and of a tube in the middle
- 6th bank at the wall and in the middle
- 11th bank at the wall and in the middle.

Three measuring tubes with different elastic characteristics were used. The Re-number (referred to the flow velocity ahead of the bundle and to the tube diameter) was appr. 50.000 for all experiments. The power spectral densities were determined as a function of the Strouhal number being the usual dimensionless number for vibrations due to fluid flow. The Strouhal number $S = \frac{fd}{v}$ in which d = tube outer dia, v = flow velocity ahead of the tube bundle and f = frequency.

3.1.2. Results of measurements with a stiff measuring tube.

The first series of tests was carried out with a relatively stiff measuring tube having a natural frequency of 75 Hz.

In summary the main conclusions for the tests with the measuring tube at the locations mentioned in the previous chapter are:

a. The fluctuating forces are of a random nature.

b. When either of the two turbulence producing perforations are installed upstream of the bundle the highest level of fluctuating forces is found in the 6th tube bank - in general probably in the 3rd to the 8th bank.

c. Concerning the shape of the spectra of the fluctuating forces, in the 1st bank essentially continuous spectra were measured leveling-off to practically zero at a Strouhal number $S = \frac{fd}{v}$ of 1.
In the 6th bank a relatively sharp and high-intensity peak (random narrow-band type) was observed around a Strouhal number of about 1.
In the 11th bank the level of excitation was less than in both the 1st and 6th row.

+) Remark: Nomenclature: Tubes which are lined up in a row in the direction of the flow are referred to as a row of tubes. Tubes which are adjacent perpendicular to the direction of the flow are referred to as a bank of tubes.

3.1.3. Measurements with elastic measuring tubes.

In order to establish whether the elastic characteristics of the tubes might have an influence on the fluctuating forces and whether synchronization of vortex shedding could occur, a second series of measurements was carried out with measuring tubes with natural frequencies of 48,6 and 34,4 Hz. These measurements were carried out in the 6th bank where the level of fluctuating forces was found to be the highest in the previous measurements. With respect to the turbulence characteristics of the flow upstream of the bundle the measurements were confined to the scaled-up steam-generator grid.

The main conclusions are:

a. The random characteristics of the fluctuating forces are confirmed.

b. Synchronization of vortex shedding is well known for bundles of parallel tubes in cross flow is not likely to occur in tube banks of counterwound helical tubes under the flow conditions of the SNR-300 steamgenerators.

3.2. Response analysis of helical-coil tube-bundle.

The bundle consists of various layers of helical tubes, supported by vertical tie-bars. The natural frequencies associated with local tube vibration are then well above the excitation frequencies.

Since the manufacturing process for the evaporator required some clearance between the various concentric sub-bundles the entire tube-bundle may have natural frequencies within the flow induced excitation frequency spectrum. It is therefore necessary that the natural frequencies and vibration modes of the entire tube-bundle and the response on the random excitation forces will be calculated in the design stage in order to establish whether dangerous flow induced vibrations can occur.

An accurate response analysis can only be carried out if accurate information about the damping of the structure is available. Therefore, measurements were carried out on an existing test bundle of the manufacturer.

3.2.1. Finite element model of tube-bundle.

The finite element model of the test tube-bundle is shown in Fig. 9.

The n layers of tubes were replaced by one helical-coiled tube with a stiffness, and mass that is n times as large as the values for the individual tubes. The 6 tie-bars were taken into account by beam elements and rigidly connected with the beam elements representing the helical-coiled tubes. For simplicity of the finite element model the vertical parts of n tubes (n=9 for the test bundle), which pass through the tube sheets were replaced by 6 tubes with a stiffness and mass n/6 times as large as for the individual tube. The tubes are assumed simply supported by the tube sheets. The entire model was built-up from 17 identical subnets, through which the input data and computercosts were considerably reduced. A subnet consisted of one thread of the helical-coiled tube, provided with 6 support bars. In a subnet the coiled tube was approximated by 24 beam elements, so that the geometry was accurately represented (See Fig. 9).

The subnets are coupled to each other with the connecting points of tubes and tie-bars. The subnets together form the main net with 109 nodal points with 6 degrees of freedom per node, being the x, y and z-displacements and the rotations about the x, y and z-axis. For the calculation of the natural frequencies and vibration modes the number of degrees of freedom was further reduced to the x- and y-displacements of the main net nodal points by the well known condensation process for stiffness and mass-matrix of the structure.

Because this model gave sufficiently accurate results the same modeling techniques were used for other sub-bundles.

3.2.2. Natural frequencies and vibration modes.

The natural frequencies and vibration modes were calculated with the ASKA-programme.[2]

Figure 10 shows the calculated and measured natural frequencies and vibration modes associated with lateral vibration of the entire bundle.

The first and second natural frequency belong to vibration modes in two perpendicular directions.

The third and sixth natural frequency, belonging to torsional vibration modes of the entire bundle, are not sensitive for flow induced excitation. Vibration modes 4, 5, 7, 8 and 10 are again lateral vibrations of the tube-bundle.

The 9th vibration mode appeared to be a rather complicated mode, showing overall lateral vibrations, torsional vibrations and local vibrations.

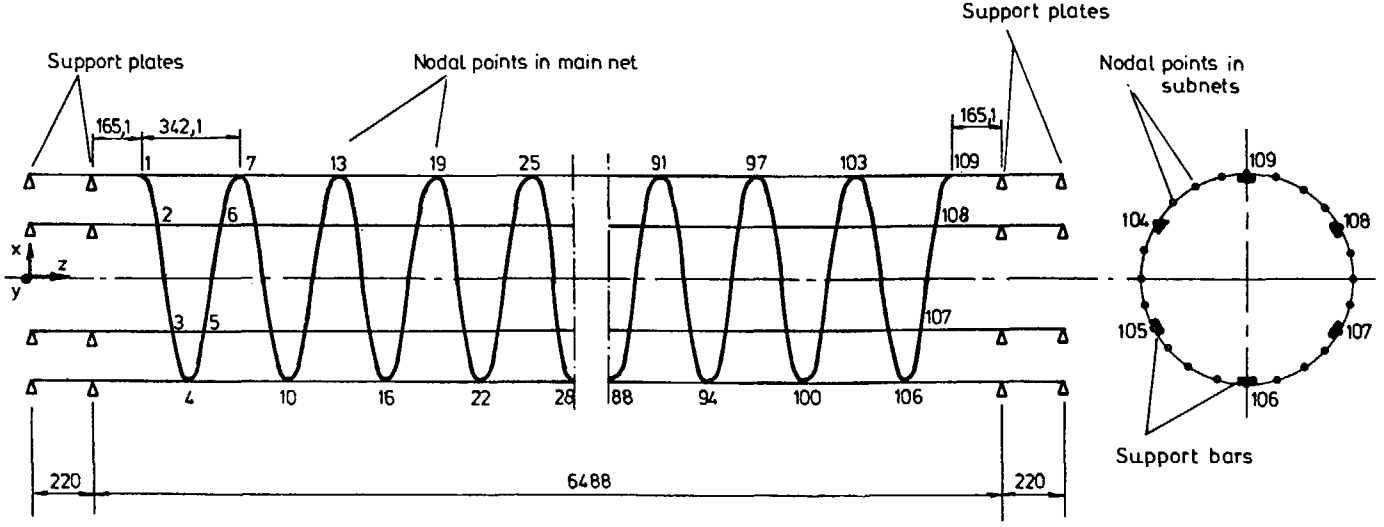

Figuur 9

Model of testbundle with helically coiled tubes, provided with support bars.

A comparison of the calculated and measured natural frequencies shows that the higher natural frequencies are more accurately predicted than the lower ones. Moreover, for the 7th and 8th natural frequency, laying close together, only one natural frequency was found experimentally.

Figure 10 shows that the experimentally obtained vibration modes are not entirely symmetric or anti-symmetric with respect to the middle of the bundle. Moreover, significant differences are observed at the lower end of the tube-bundle. These differences can be caused by the approximations made at both ends of the bundle, where the vertical tubes pass through the tube-sheets. The achieved results are however, sufficiently accurate for the response analysis, so that the element model need not to be refined.

3.2.3. Determination of the damping.

The damping of the tube-bundle, vibrating in the sodium flow, will consist of:

- structural damping
- hydrodynamic damping.

The structural damping is dependent on the vibration mode and is determined experimentally for the test-bundle. The values for the structural damping are given in Table 4 as fractions of critical damping for each vibration mode.

The liquid will also exert damping forces or the structure. It can be shown [1], that the damping force exerted on the tube can be approximated by:

$$q_r = - c_D' . \tfrac{1}{2} \rho d V' . \dot{u}_r \quad , \qquad (3)$$

where

q_r = radial force per unit length exerted on the tube

c_D' = drag coefficient based on the flow velocity between the tubes

ρ = density of fluid (sodium)

d = outside diameter of tube

V' = flow velocity between the tubes

$\dot{u}_r$ = radial velocity of the tube.

It can be seen that the hydrodynamic damping is a viscous damping per unit length of the tube.

With expression (3) and the measured drag coefficient the damping values for each vibration mode were calculated. The damping values are given in Table 4 as fractions of the critical damping.

It can be seen that the hydrodynamic damping is particularly important for the lower natural frequencies and decreases with the frequency. The structural damping increases with the natural frequency so that the total damping varies only slightly over the frequency range.

3.2.4. Response analysis and results.

For the response analysis of the tube-bundle a few assumptions have to be made.

(1) The spectra of the flow induced forces on the tubes of the banks behind the 11th bank are identical with the measured spectrum on the 11th bank.

(2) The fluctuating forces are assumed only correlated over a length equivalent with the tube length in the experimental model.

(3) The fluctuating forces on different tubes are fully uncorrelated.

(4) The forcing power spectrum is fairly uniform in the vicinity of each natural frequency.

With these assumptions, which are all realistic, the rms-value of the displacement of the tube-bundle can readily be calculated for each vibration mode. [3]

Table 2 shows the mean-square value for the maximum displacement of each vibration mode. It is clear that the tube-bundle will vibrate mainly with frequencies in the vicinity of the lowest natural frequencies for vibration in the x- and y-direction. The maximum displacement can be expected at half height of the bundle.

The rms-value for the displacement in x-direction at half height of the bundle appeared to be:

$$\langle u \rangle = 0.025 \text{ mm}$$

Calculations of the other subbundles showed that the maximum displacements are to be expected for the outer tube-bundle.

It can be concluded that the natural frequencies of the helical coiled tube-bundle are so low that due to the flow induced fluctuating forces the tube-bundle will show a narrow band random vi-

Figuur 10 Vibration modes of testbundle

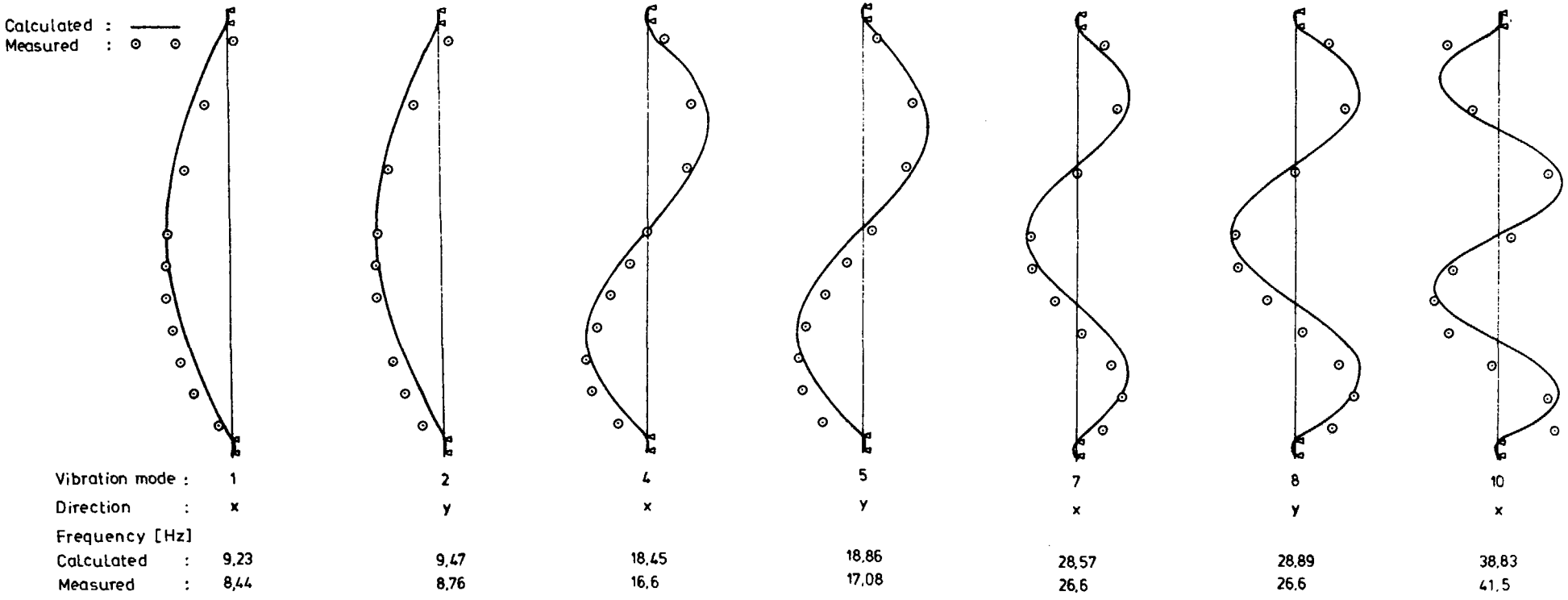

NATURAL FREQUENCIES, DAMPING AND CALCULATED VARIANCE OF MAXIMUM DISPLACEMENT FOR VARIOUS VIBRATION MODES OF A TUBE-BUNDLE

TABLE 3

Vibration mode	Natural frequency f_k (Hz)	Dimensionless natural frequency $S_k = \frac{f_k . d}{V}$	Measured structural damping ζ_m	Calculated hydrodynamic damping ζ_h	Total damping ζ_k	Dimensionless power spectral density $\frac{f_k K_y(f_k)}{\bar{K}_x^2}$	Variance of displacement $\langle u_{max}^2 \rangle$ (m^2)
1	8.468	0.3996	0.0036	0.0099	0.0135	0.011	5.840×10^{-10}
2	8.685	0.4099	0.0045	0.0097	0.0142	0.011	5.828×10^{-10}
4	16.923	0.7986	0.0036	0.0050	0.0086	0.022	1.409×10^{-10}
5	17.303	0.8166	0.0045	0.0048	0.0093	0.022	1.127×10^{-10}
7	26.211	1.2370	0.0063	0.0032	0.0095	0.012	1.855×10^{-11}
8	26.502	1.2507	0.0063	0.0032	0.0095	0.012	1.124×10^{-11}

bration with a frequency that varies slightly about a mean value correponding to the lowest natural frequency.

The magnitude of the vibrating displacements however, will remain very small due to the random nature of the flow induced fluctuating forces and the structural and hydrodynamic damping of the tube-bundle.

3.3. Measurements on prototype (50 MW).

Measurements are carried out on the outside of the outershell by means of 3 accelerometers. The first was placed at the height of the upper tube plate. The second in the middle of the shell. The third on the lower side of the shell. The measured amplitudes were very small (10^{-8}m). The goal of these measurements was loose part detection and leakdetection.

Other measurements were carried out on 3 tubes. For these measurements the following instrumentation was mounted:

- an accelerometer, mounted on a tube, at the inflow side, at the position where the tube turns from vertical into horizontal direction.
  Selected is the tube with the largest length between the tube supports.
- two strain gauges point welded on the tubes.
  One gauge was placed beside the accelerometer, the signals could be compared.
  The second gauge was on the sixth row from the top.

The following results were obtained with these measurements:

- The measurements with strain gauges were presented by power spectra. The highest strain amplitudes are measured with a frequency of 2 Hz and a peak value of 1.7×10^{-6} which is mainly the influence of flow fluctuating in the tubes. The amplitudes are very small. With a temperature of 400 °C the resulting stress will be 0,3 N/mm^2.

  From the power spectra of the accelerometer followed that the highest acceleration amplitude is 1.33×10^{-3} m/s^2 with 14.3 kHz and full load SNR evaporator conditions.

  The resulting stresses are negligible.

The calculated response of the entire bundle could not be found, because the manufacturing process for the prototype causes no clearance between the different sub-bundles. Consequently no resonance vibrations can occur.

4. THE INTERMEDIATE HEATEXCHANGER (IHX)

The sodium-sodium heatexchanger or intermediate heatexchanger (IHX) is designed to protect the reactor against damage resulting from a steam-generator accident, for example a sodium/water reaction. Furthermore, radio-active sodium should be prevented from penetrating into non-radio-active systems or into the environment.

The system requirements, resulting in a design having vertical straight tubes and a floating head as shown in Fig. 11. A modular concept was chosen so as be able to meet the requirement for withstanding high accident pressures.

The primary sodium flows in parallel around the tubes; the secondary sodium enters through a central tube and flows upwards through the tubes. If required, the tube bundle can be lifted out of the shell.

TABLE 4
MAIN DIMENSIONS OF IHX

Tube diameter x wallthickness	21 x 1.4	mm
Tube length between tube-plates	7.6	m
Number of tubes	846	
Diameter of central tube	400	mm
Vessel diameter	1360	mm
Overall height	12.8	m
Nozzle diameter	300	mm
Tube support distance	770	mm

TABLE 5
WORKING DATA OF IHX

Capacity	85	MWth
Primary outlet temperature	375	°C
Primary inlet temperature	546	°C
Primary flow	392.6	kg/s
Secondary inlet temperature	335	°C
Secondary outlet temperature	520	°C
Secondary flow	562.5	kg/s
Working pressure on primary side	11.2	bar
Working pressure on secondary side	11.8	bar.

4.1. Measurements on prototype THX.

a) Tube measurements.

Measurements are prepared on tubes, for which 4 accelerometer units are developed. Each unit is mounted in a tube before the component is installed.

The units are fixed on the lowerside of the tubes by means of sliding springs. The units can be moved upwards by pulling on the thin tubes, mounted on the units and quided through nozzles on the upper side of the component.

In this way at several places of the tubes can be measured: outlet region, between 2 tube-supports, at the location of a tube support and inlet region.

For each location measurements are carried out for several primary sodium flows: 30, 50 and 100 %.

The measurements will be carried out end 1977.

b) Measurements on inner- and outer shell of the component.

On the innershell accelerometers are mounted to measure the vibrations at upper and lowerside of the innershell in two perpendicular directions. Also an accelerometer on the lowerside of the outershell has been placed.

For different sodium flows the vibrations will be measured end 1977.

5. CONCLUDING REMARKS

(1) It can be concluded that the necessary clearance of the tubes in the support plate holes of the straight tube steamgenerator may cause some resonance frequencies. The vibrational amplitudes however will remain very small, because of the small fluctuating forces, the damping in the support-grid holes and the hydrodynamic damping. The experiment with the prototype steamgenerator confirmed the conclusions based on the theoretical analysis.

(2) The helical-coil steamgenerators have stiff connections between tubes and support-bars and consequently no local vibrations are to be expected. It has been shown that in case the various concentric bundles have some radial clearance, the natural frequencies of the entire bundle may come within the excitation frequency spectrum, but the vibration amplitude will remain very small, due to the random nature

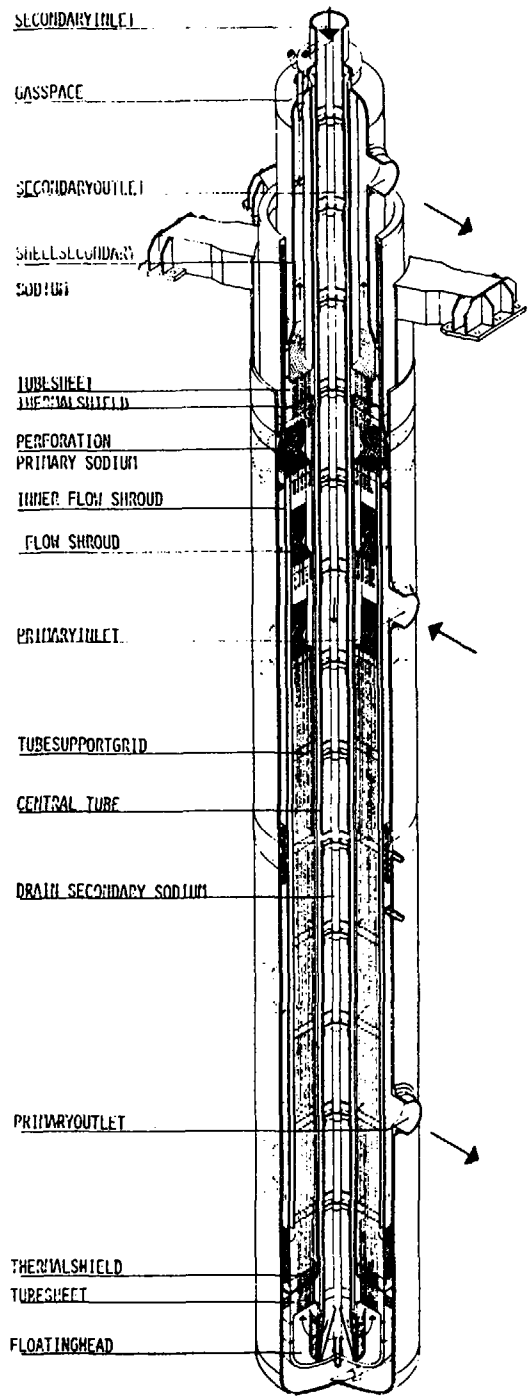

Figure 11
85 MW INTERMEDIATE HEAT EXCHANGER SNR 300

of the excitation forces and the structural and hydrodynamic damping of the bundle.

(3) The vibrational behaviour of the tubes of the IHX will be determined experimentally with the prototype heatexchanger.

Acknowledgement

The work described here forms part of a government financed project aimed at the development of heat transfer components for SNR-300.

The experimental research described in this paper was carried out at Central Technical Institute TNO at Apeldoorn.

The author is very grateful to the Project Group for Nuclear Energy TNO and to B.V. Neratoom for the cooperation in the preparation of this paper.

References

[1] NAUDASCHER, E.
Flow Induced Structural Vibrations.
IUTAM-IAHR Symposium, Karlsruhe 1972.

[2] ASKA PART II - LINEAR DYNAMIC ANALYSIS.
User's reference manual, ISD, Stuttgart, 1974.

[3] CRANDALL, S.H.
Random vibration, volume 2.
The M.I.T. Press.
Cambridge, Massachusetts, 1963.

A Review of ANL Base Technology Studies in Support of the U.S. LMFBR Vibration Program by M. W. Wambsganss, S. S. Chen, T. M. Mulcahy and Y. S. Shin, United States.

ABSTRACT

Argonne National Laboratory (ANL) is the center for base technology studies of flow induced vibration for the U.S. LMFBR Program. This paper reviews and summarizes published results, reports on the status of ongoing programs, and discusses future needs as outlined in the U.S. LMFBR Vibrations Program Plan.

INTRODUCTION

The U.S. LMFBR Vibration Program Plan includes three major areas of activities designated as Base Technology, Applied Technology, and Methods Evaluation. Very briefly, the objectives of each of these areas of work can be defined as follows:

Base Technology: To develop new and/or improved methods of analysis and testing, satisfying technological needs identified by reactors designers/analysts, and to incorporate these methods into design guides.

Applied Technology: To apply state-of-the-art methods of analysis and testing in the design development and evaluation of specific reactor components.

Methods Evaluation: To utilize results from pre-operational and operational tests of LMFBRs to evaluate analysis and test methods, thereby leading to validation and/or refinement of design guides.

Applied technology activities have been carried out in support of the Fast Flux Test Facility (FFTF) [1] and Clinch River Breeder Reactor (CRBR) [2] Projects. These activities have included design reviews, for the purpose of identifying potential vibration problem areas, followed by state-of-the-art analyses and tests of specific components. In attempting to evaluate a given design using analytical methods, it soon becomes apparent that state-of-the-art methods, despite a continuing improvement in the understanding of basic phenomena related to flow induced vibration, are generally inadequate. Consequently, it has been necessary to rely heavily on development testing, including feature, scale-model, and prototypic tests. However, testing is both time-consuming and expensive; it is difficult to make extensive parameter studies; and extrapolation from model tests to the prototype is not well established. These factors (the inadequacy of state-of-the-art methods of analysis and the high cost and limitations of testing) point up the need for studies of a base technology nature designed to advance the state-of-the-art.